



OPEN

SUBJECT AREAS:

BIOANALYTICAL
CHEMISTRYELECTRONIC PROPERTIES AND
MATERIALSReceived
23 December 2013Accepted
5 March 2014Published
21 March 2014Correspondence and
requests for materials
should be addressed to
J.J.X. (xujj@nju.edu.cn)
or H.Y.C. (hychen@
nju.edu.cn)

Bismuthoxyiodide Nanoflakes/Titania Nanotubes Arrayed *p-n* Heterojunction and Its Application for Photoelectrochemical Bioanalysis

Wei-Wei Zhao¹, Zhao Liu², Shu Shan¹, Wen-Wen Zhang², Jing Wang¹, Zheng-Yuan Ma¹, Jing-Juan Xu¹ & Hong-Yuan Chen¹¹State Key Laboratory of Analytical Chemistry for Life Science, School of Chemistry and Chemical Engineering, Nanjing University, Nanjing 210093, China, ²Department of Vascular Surgery, Nanjing Drum Tower Hospital, the Affiliated Hospital of Nanjing University Medical School, Nanjing 210008, China.

We have developed sensitive detection of cancer biomarker vascular endothelial growth factor (VEGF) using the *p-n* heterojunction comprised of *p*-type BiOI nanoflakes (NFs) array and *n*-type TiO₂ nanotubes (NTs) array. Due to the unique arrayed structure and the synergy effect of photoelectrochemistry in the formed *p-n* junction, the synthesized configuration has superior excitation efficiency and thus excellent photoresponsibility. Then, the fabricated *p-n* heterojunction was integrated with an exquisite bioassay protocol for addressing VEGF using a sandwich immunoassay with glucosedehydrogenase (GDH) as the enzyme tags. Due to the excellent performance of BiOI NFs array/TiO₂ NTs array and the ingenious signaling mechanism, the proposed system could achieve the sensitive and specific VEGF detection. This work not only presents a simple BiOI NFs array/TiO₂ NTs array *p-n* heterojunction for general applications in the broad photochemistry areas, but also opens a different horizon for current development of advanced PEC biomolecular detection.

The newly emerged photoelectrochemical (PEC) bioanalysis has rapidly becoming a current research hotspot due to its desirable properties and attractive potential in future bioassay^{1–20}. From the very beginning of such technique, the exploitation of various functional semiconductive materials and its utilization for advanced bioanalytical protocols has been a focus of substantial research since these efforts would probably underlie elegant routes for probing biological events. Of late, nafion-functionalized CdS–methyl viologen quantum dots (QDs) was equipped on ITO electrode for the ultrasensitive PEC detection of cysteine⁴. More recently, ZnO/ZIF-8 nanorods architecture was successfully synthesized and examined for selective PEC chemosensing⁹. Soon afterwards, IrO₂–Hemin–TiO₂ nanowire arrays was proposed for the sensitive PEC detection of glutathione¹⁰. Although these previous work have achieved remarkable results, the investigation on this field is still in its early stage due to the short development time and new versatile semiconductive electrode is yet of urgent need for application in advanced PEC biomolecular detection.

With unique photophysical features, semiconductor heterostructures have been a highly exploited subject in a plethora of areas^{21,22} including photocatalyst or solar cells. For example, CdS/Cu₂S *p-n* junction nanowire was fabricated for efficient photovoltaic cells²³. The CdS/CuGaSe₂ *p-n* junction was successfully synthesized for stable PEC hydrogen evolution²⁴. However, such *p-n* junction architecture has seldom been exploited for PEC bioanalysis application. Obviously, to develop new *p-n* junction with unique structure and/or enhanced properties would be desirable for application in future PEC analysis.

As known, numerous TiO₂ nanostructures have long been used for bioanalysis purposes due to their good biocompatibility and chemical/thermal stability as well as environmental benignity. In particular, the TiO₂ nanotubes (NTs), a well-known *n*-type semiconductor (with band gap of ~3.2 eV) with regular oriented structure and high surface area, has received much attention due to its outstanding merits in manifold fields including PEC detection. We previously had exploited CdS QDs/TiO₂ NTs hybrid for PEC bioassay application¹⁷. BiOI is an attractive ternary *p*-type semiconductor with a narrow band gap (~1.8 eV) and strong absorption in the visible region (with absorption edge of ~680 nm) which currently begins its career in the field of photocatalysis^{25–27}. In



fact, comparing with other semiconductive materials, to date there is surprisingly little research on BiOI in spite of its interesting PEC properties²⁸. So, of particular interest here is the possibility of developing a new BiOI/TiO₂ *p-n* junction heterostructure and using as a versatile visible-light-active hybrid for biomolecular detection purposes. If possible, such hybrid is supposed to possess great advantages due to their synergic effect and harnessing this type material would in principle allow the operation of PEC detection with higher efficiency, the success of which could provide great opportunities for further biosensing construction.

In this work, we for the first time fabricated a simple and versatile *p-n* heterojunction architecture comprised of BiOI crossed nanoflakes (NFs) array/TiO₂ NTs array, which was then exploited for advanced PEC biomolecular detection toward vascular endothelial growth factor (VEGF), an important cancer biomarker for breast cancer, lung cancer, colorectal cancer, as well as rheumatoid arthritis. Structurally, as illustrated in Figure 1A, the synthesized hybrid was expected to function as a “light collector”, i.e., the *p*-type BiOI NFs array with large surface area could facilitate the efficient light harvesting while the *n*-type TiO₂ NTs array would provide an effective directional pathway for rapid electron transportation. Significantly, the distinct photoelectrochemistry in the formed *p-n* junction would behave like a spontaneous “exciton pump” that additionally is advantageous for the resulting performance. As shown in Figure 1B, the BiOI NFs array/TiO₂ NTs array was then used for VEGF detection by an ingenious PEC immunoassay protocol. In detail, after anchoring the first antibodies via the chitosan-glutaraldehyde (CS-G) bridging, an immunosandwich assembly was formed on the bifunctional electrode with glucosedehydrogenase (GDH) as the enzyme tags through the biotin-streptavidin (B-SA) affinity system (experimental details see the ESI). The subsequent reaction of the GDH with glucose substrate in the presence of its NAD⁺ cofactor would lead to the enzymatic product of NADH, which could neutralize the holes localized on *p*-type BiOI and hence boost charge separation and photocurrent generation. In such system, increased VEGF concentration leads to the enhanced GDH loading and thus promotes the NADH generation for improved photocurrent

responding. Due to the excellent performance of BiOI NFs array/TiO₂ NTs array and the exquisite signaling mechanism, the proposed system could achieve the sensitive and specific VEGF detection. To the best of our knowledge, both the fabricated BiOI NFs array/TiO₂ NTs array structure and the proposed PEC bioanalytical strategy have never been reported.

Results

Experimentally, to achieve the hierarchical structure of designed BiOI NFs array/TiO₂ NTs array, successive ionic layer adsorption and reaction (SILAR) was used to build the BiOI array onto the TiO₂ NTs fabricated by electrochemical anodization firstly. Such direct SILAR growth of BiOI flake membranes onto TiO₂ NTs can be performed at room temperature, atmospheric pressure with good convenience and repeatability. Specifically, the self-organized TiO₂ NTs were grown by anodization of Ti foils in a 0.5 wt% hydrofluoric acid solution at 20 V for 60 min. Thereafter, BiOI NFs were coated onto the TiO₂ NTs by alternately immersing the latter into two different ionic precursor solutions containing Bi³⁺ and I⁻ ions, respectively (experimental details see supporting information). Figure 2A shows a typical scanning electron microscopy (SEM) image of the as-obtained self-organized TiO₂ NTs, which exhibited a one-dimensional (1D) perpendicularly aligned and highly ordered porous structure. A high-magnification SEM image further displayed that the average inner and outer pore diameter were ca. 100 and 140 nm, respectively. Figure 2B demonstrates the morphology of the three-dimensional (3D) crossed BiOI NFs on TiO₂ NTs, it possessed unique layered structures (with lateral dimension in the micrometer size, height of several hundred nm and average thickness of ca. 10 nm, as shown in Figure 1B inset) with the internal static electric field perpendicular to each layer, which can induce the effective separation of photo-generated electron-hole pairs. Figure S1 and S2 provides insight into the effect that the SILAR cycles have on the location and growth density of crossed BiOI NFs on TiO₂ NTs. X-ray photoelectron spectroscopy (XPS) was further performed to study the surface chemical compositions and oxidation states of BiOI NFs/TiO₂ NTs. The obtained survey spectrum is depicted in Figure 2C,

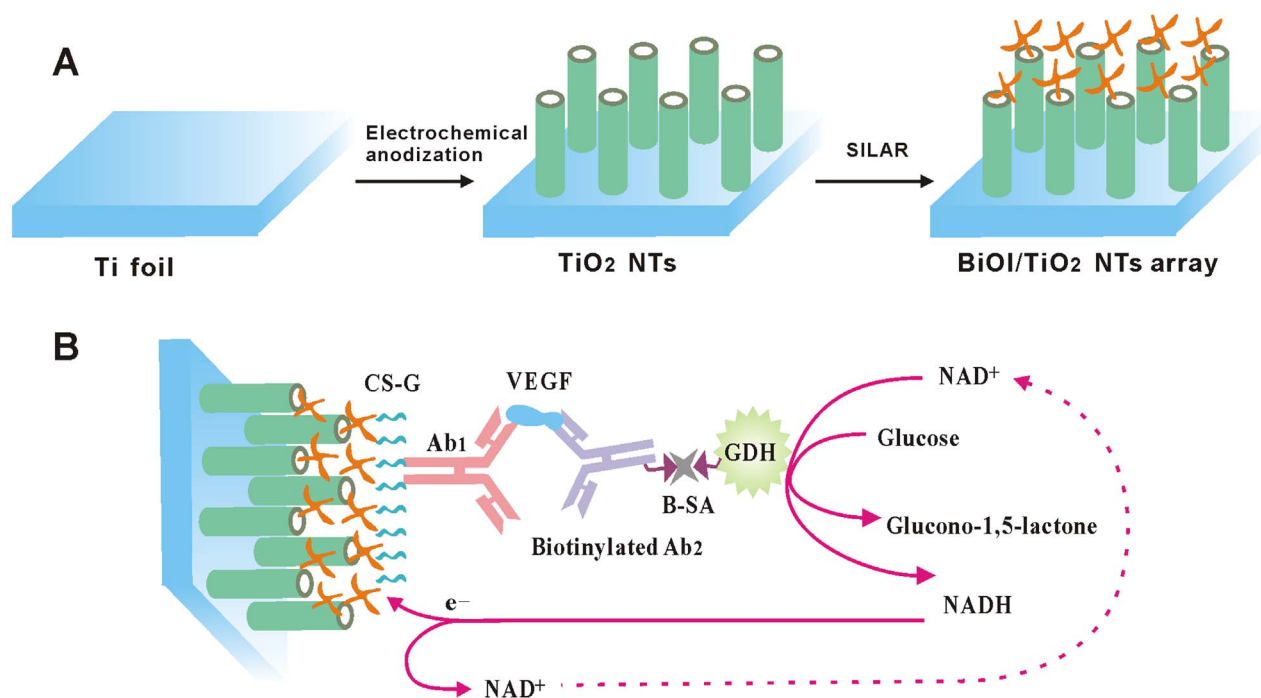


Figure 1 | (A) Schematic Illustration for fabricating crossed BiOI NFs/TiO₂ NTs arrayed structure. (B) Schematic diagram of the immunoanalysis principle using the novel BiOI/TiO₂ NTs arrayed *p-n* junction photoelectrode.

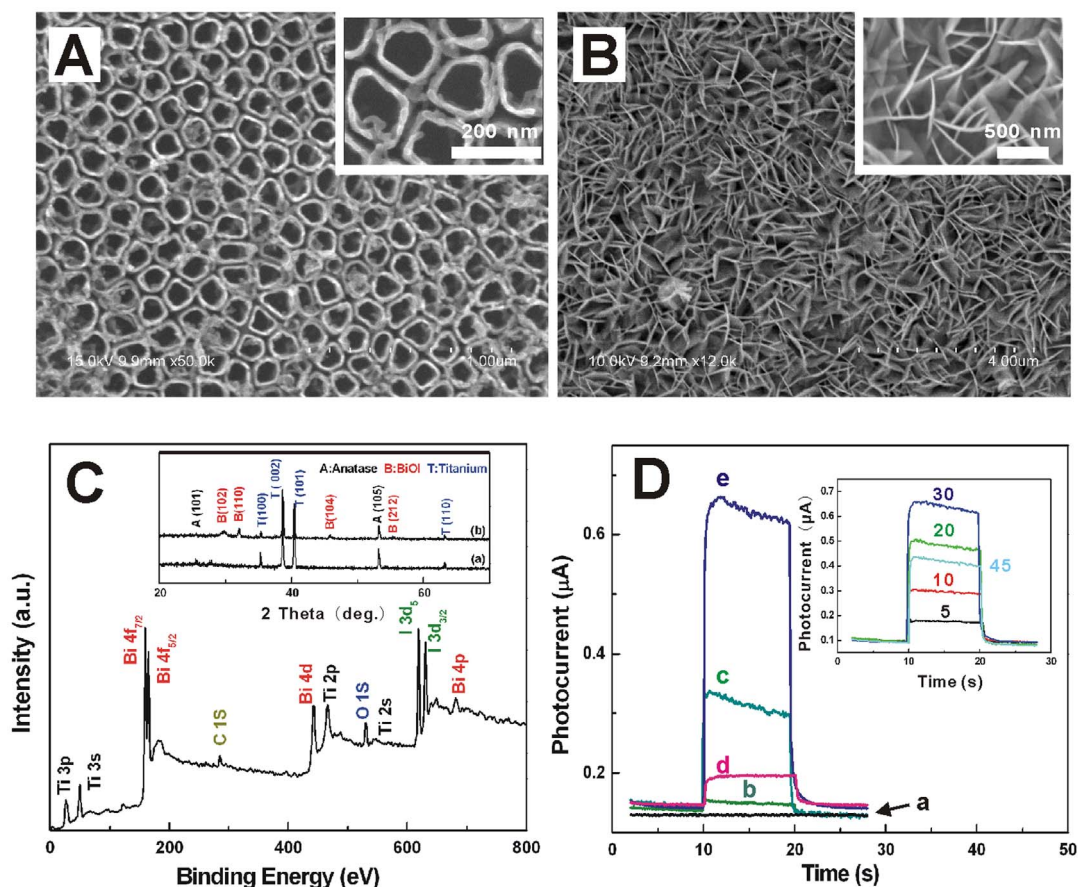


Figure 2 | (A) SEM of the self-organized TiO₂ NTs, the inset: high-magnification SEM image (B) SEM of the 3D interlaced network of BiOI layer on TiO₂ NTs, the inset: high-magnification SEM image, (C) XPS spectrum of the hybrid, the inset: XRD pattern of the developed TiO₂ NTs (a) and BiOI/TiO₂ hybrid (b), (D) Transient photocurrent response of the samples, the bare Ti foil (a), the TiO₂ NTs (b, d) and BiOI/TiO₂ hybrid (c, e) in 0.10 M tris-HCl (pH 7.8) without (b, c) and with (d, e) 1.0×10^{-3} M NADH, the inset: the effect of SILAR cycles of BiOI on the resulting hybrids. All photocurrent responses were recorded with 0 V working potential and 470 nm light wavelength on and off.

and the corresponding high-resolution XPS spectra of Bi 4f, O 1s and I 3d are illustrated and discussed with Figure S3. The phase structure of the sample was further identified by X-ray diffraction (XRD), as shown in Figure 2C inset, quantitative analysis of the pattern would index all the observed peaks to the TiO₂ anatase phase (JCPDS file No: 21-1272, $a = 3.7852$ Å, $c = 9.5139$ Å, space group: $I4_1/amd$ (141)), tetragonal structure of BiOI (JCPDS file No: 10-0445, $a = 3.994$ Å, $c = 9.149$ Å, space group: $P4/nmm$ (1129)), and the Ti metal phase (JCPDS file No: 44-1294, $a = 2.951$ Å, $c = 4.683$ Å, space group: $P63/mmc$ (194)), respectively, suggesting that no Bi and I related impurities exist in the BiOI/TiO₂ NTs hybrid. Transient photocurrent responses of the samples were also investigated upon intermittent visible light irradiation of 470 nm with the results shown in Figure 2D. As shown in curve a, the Ti foil exhibited no photoresponse. In contrast to the weak response of bare TiO₂ NTs (curve b), the absolute intensity (the illuminated current subtracts dark current) of such novel array-array heterostructure (curve c) enhanced greatly from 1.0×10^{-8} to 1.67×10^{-7} A, indicating the strong coupling effect between BiOI NFs and TiO₂ NTs. Significantly, comparing curve e and c, we would find that the presence of electron donor nicotinamide adenine dinucleotide (NADH) in the solution can greatly amplify the response of the samples, indicating that NADH can neutralize the generated holes and hence contribute to the photocurrent production. Figure 2D inset shows the effect of SILAR cycles of BiOI on the resulting hybrids, with the increased loading of BiOI on the TiO₂ NTs up to 30 cycles, the response of the hybrid enhanced correspondingly. Further increase of the SILAR cycles to 45 cycles led to the signal reduction, which

may be caused by the too dense distribution of BiOI NFs that impaired interfacial mass and electron communication.

For comparison, other two structures composed of BiOI NFs on TiO₂ nanoparticles (NPs) film on indium tin oxide (ITO) electrode (BiOI NFs/TiO₂ NPs/ITO) and BiOI coating on TiO₂ NTs tube wall (BiOI coating/TiO₂ NTs) were then constructed (experimental details see ESI). Figure 3A depicts the SEM images of the as-prepared samples. As shown, in the two samples, optimized TiO₂ NPs film¹⁴ (Figure 3A-a) and BiOI coating²⁶ (Figure 3A-d) were used in place of the TiO₂ NTs array and the BiOI NFs array, respectively. To clarify how the architecture affects the performance, Figure 3B demonstrates the photocurrent responses of all the three samples under visible-light irradiation of 470 nm. As shown, compared to BiOI coating/TiO₂ NTs, the outstanding behavior of BiOI NFs/TiO₂ NTs could be attributed to the presence of NFs structure that permits higher efficiency of light harvesting. As to the difference between the TiO₂ NPs and TiO₂ NTs-based samples, although 1D architectures also change how the film absorbs light, the primary mechanism for improvement is the enhanced residence lifetime²⁹. To further pinpoint how BiOI species are contributing to broadband photocurrent, the incident-photon-to-carrier efficiency (IPCE) is then determined by using the expression (1):

$$\text{IPCE}(\lambda) = \frac{1240 \times I_{sc}(\lambda)}{\lambda \times I(\lambda)} \times 100\% \quad (1)$$

where $I_{sc}(\lambda)$ is the wavelength dependent short-circuit photocurrent density in A/cm², $I(\lambda)$ is the wavelength dependent incident light intensity in W/cm², and λ is the excitation wavelength in nm.

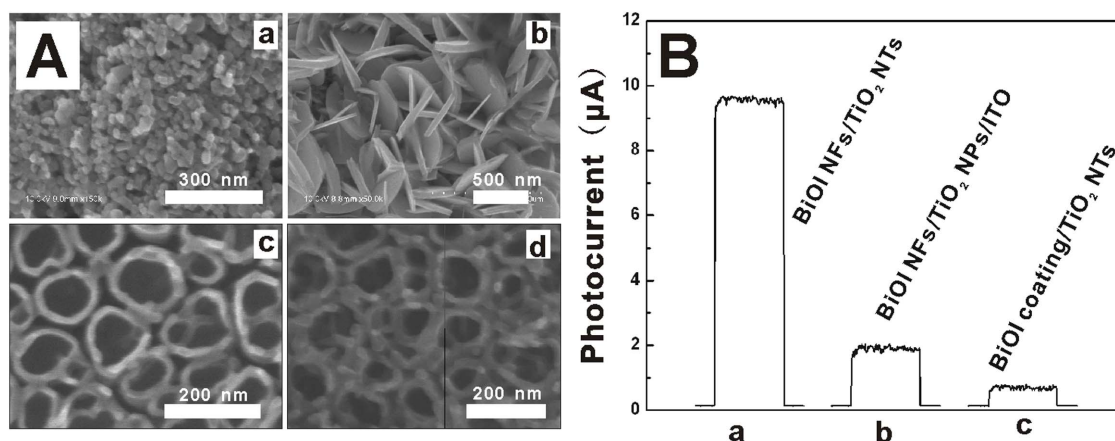


Figure 3 | (A) SEM images of the as-prepared (a) TiO₂ NPs film, (b) BiOI NFs/TiO₂ NPs/ITO, (c) TiO₂ NTs, (d) BiOI film/TiO₂ NTs. (B) The photocurrent responses of the (a) BiOI NFs/TiO₂ NTs, (b) BiOI NFs/TiO₂ NPs/ITO, (c) BiOI coating/TiO₂ NTs. All the tests were performed in 0.10 M PBS containing 0.10 M ascorbic acid with 0 V working potential and 470 nm excitation light.

Upon analysis, the results of 25.3%, 5.01% and 1.79% were obtained for BiOI NFs/TiO₂ NTs, BiOI NFs/TiO₂ NPs/ITO and BiOI coating/TiO₂ NTs, respectively. Incidentally, the IPCE 5.01% of the sample BiOI NFs/TiO₂ NPs was near the 4% of a similar structure on fluorine-doped tin oxide (FTO) electrode³⁰. These value further identified that the superior performance of the proposed hybrid was of intimate relevance to the proposed arrayed structure.

Apparently, due to its unique configuration and property, the developed *p-n* heterojunction has great potential for application in the broad field of photochemistry such as photocatalysis or solar cells. As mentioned above, here its opportunity to the important field of molecular detection was examined. As shown in Figure 1B, on basis of the developed photoelectrode, an innovative sandwich protocol was then designed for probing the immunocomplexing toward VEGF. As far as we known, GDH has never been used as enzymatic labels for PEC detection before. Previous experiment had demonstrated that the response of the developed photoelectrode could be obviously enhanced by NADH. Figure 4A manifests the photoresponse of the immunosystem to VEGF at a level of 1.0×10^{-6} g/mL in the absence and presence of glucose (10 mM). As expected, in the absence of glucose, the response of the system was weaker (curve b) than that of the bare hybrid electrode (curve a), which related to the formation of insulating protein layer that

affected the efficient hole scavenging. By contrast, in the presence of substrate, the system exhibited enhanced photoresponse (curve c), which could be attributed to that the existence of glucose could *in situ* induce NADH production and thus the attenuated charge recombination. Apparently, the signal intensity correlates intimately with VEGF concentration; our preliminary results have shown that the VEGF determination can be accomplished by following the signal variation. As shown in Figure 4B, the signal climbs along with the VEGF concentration ascends up to 1.0 ng/mL, and the detection limit was experimentally found to be 10 pg/mL. As shown in Figure 4B inset, the selectivity was assessed by using another two head and neck squamous cell carcinoma (HNSCC) biomarkers, i.e., interleukin 6 (IL-6) and interleukin 8 (IL-8) as interfering agents, the results indicated that these interfering agents could not cause an apparent signal increase and thus the satisfactory selectivity. The reproducibility of this PEC immunoassay was then evaluated by intra-assay relative standard deviation (RSD). At the level of 1.0 ng/mL, the RSD was 7.3%, suggesting an acceptable reproducibility of the proposed protocol. The result of real plasma sample test was 82.7 pg/mL, which was slightly higher than the 76.3 pg/mL of the commercial ELISA test. These results indicated the potential of the developed immunoassay for practical applications.

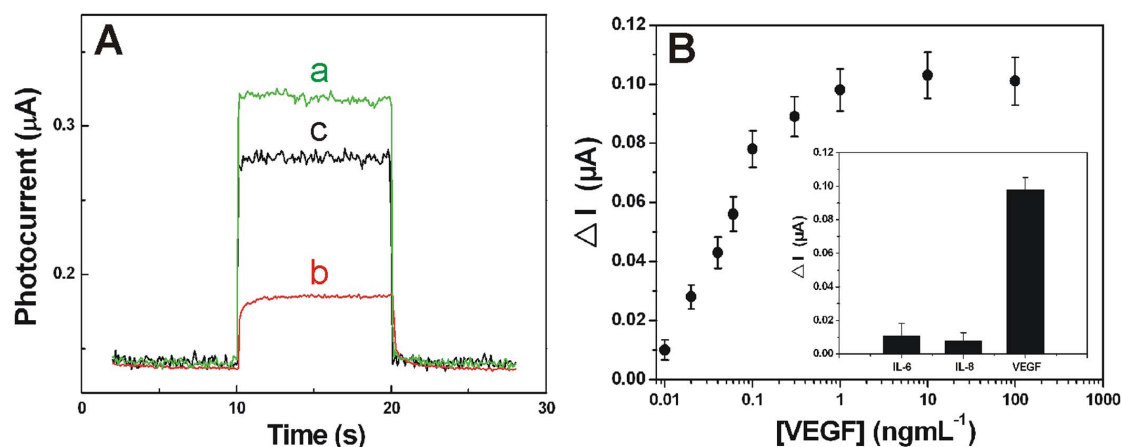


Figure 4 | (A) Photocurrent response of (a) the bare BiOI/TiO₂ NTs electrode, the developed immunosystem in the (b) absence and (c) presence of 10 mM glucose in 0.10 M tris-HCl (pH 7.8) containing 10 mM NAD⁺ cofactor (corresponding to 1.0×10^{-6} g/mL of VEGF). (B) Plot of the photocurrent vs VEGF concentration. ΔI is the photocurrent enhancement corresponding to variable VEGF concentration. Inset: Selectivity of the proposed immunoassay to VEGF by comparing it to the interfering proteins at 1.0 ng/mL, IL-6 and IL-8.

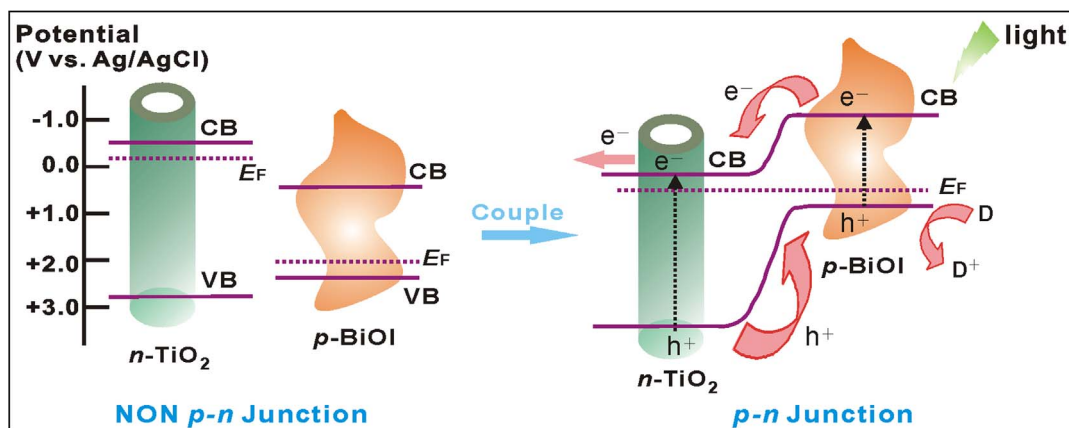


Figure 5 | Schematic diagrams for the energy bands of *p*-type BiOI and *n*-type TiO₂ before and after coupling, as well as the specific charge transfer process at the formed *p-n* junction under visible-light irradiation.

Discussion

The reasons for the excellent property of the as-fabricated electrode are threefold: (1) the arrayed architecture of the hybrid. The 3D interlaced network of BiOI layer with large surface areas would allow extended light harvesting, while the well-aligned 1D features of TiO₂ NTs array could provide an effective directional electron percolation pathway and hence the enhanced carrier mobility and lifetime¹⁷. (2) the peculiar activity of TiO₂ NTs. As known, generally TiO₂ is a wide band gap semiconductor and not photoactive under visible light illumination. However, the vertically oriented structure would endow TiO₂ NTs with distinct responsibility in a specific visible range³¹. (3) the formation of *p-n* junction. The contact of *p*-type BiOI and *n*-type TiO₂ could form the *p-n* heterojunction, rendering the rise of Fermi level and whole energy band of BiOI while the descent of those of TiO₂ till a new stable equilibrium, wherein the reformed conduction band (CB) edge of BiOI exceeds that of latter. So, when upon visible irradiation, the *p-n* junction would facilitate the effective separation and quick transportation of the photogenerated excitations. Specifically, as illustrated in Figure 5, charge separation could occur simultaneously both in BiOI NFs and TiO₂ NTs. Then, the photoelectrons of *p*-type BiOI would promptly inject into the CB of *n*-type TiO₂, while the holes of latter would transfer to the valence band (VB) of the former. These injected electrons on the CB of TiO₂ NTs were then rapidly collected by the Ti substrate as photocurrent due to the efficient charge transport within the arrayed tubes. The synergy effect of these factors could substantially promote the spatial charge separation and the subsequent migration of these carriers, impeding the charge recombination and thus improving the excitation and conversion efficiency.

The following assay confirmed the excellence of the developed *p-n* junction architecture and also the feasibility of the proposed sensing protocol. Further work will modulate the experimental conditions to optimize the property of the hybrid and exploit its utilization for other bioanalysis application. In summary, a distinct *p-n* heterojunction has been constructed on basis of coupling *p*-type crossed BiOI NFs array to *n*-type TiO₂ NTs array. Due to the unique arrayed structure consisted of 3D interlaced network of BiOI NFs layer and the 1D configuration of TiO₂ NTs, the developed hybrid possessed excellent photo-to-electric conversion efficiency. By means of an immunosandwich protocol, we further demonstrated that this hybrid enabled novel PEC biomolecular detection toward protein marker which could be extended to other biorecognition events. These results not only offered a unique BiOI NFs/TiO₂ NTs *p-n* heterojunction which has a wide application prospects in the broad photochemistry, but also opened a different perspective for current development of advanced PEC biomolecular detection.

Methods

Fabrication of the 3D BiOI Crossed NFs Array/1D TiO₂ NTs array *p-n* heterojunction electrodes. The utilized TiO₂ NTs were fabricated by the technique of electrochemical anodic oxidation according to our previous report¹⁷. In detail, prior to anodization, Ti sheets were mechanically polished with different abrasive papers and rinsed in an ultrasonic bath of cold distilled water for 10 min. Then the cleaned Ti sheets were soaked in a mixture of HF and HNO₃ acids for 1 min (the mixing ratio of HF:HNO₃:H₂O is 1:4:5 in volume). Using 0.5 wt% hydrofluoric acid as the electrolyte, the cleaned titanium sheets was anodized at 20 V at room temperature for 60 min in a conventional two-electrode system with a platinum electrode as the cathode. Anodized Ti sheets were washed with ultrapure water and then annealed at 500 °C for 1 h in ambient atmosphere to crystallize the amorphous tubes to obtain the well-ordered and uniform TiO₂ NTs array. On basis of the developed TiO₂ NTs, the 3D BiOI crossed NFs array/1D TiO₂ NTs array *p-n* heterojunction electrode was then prepared by a successive ionic layer adsorption and reaction (SILAR) approach. Briefly, before use, the TiO₂ NTs substrates were cleaned by ultrasonication in distilled water and ethanol, subsequently. Then, BiOI flakes were coated onto the TiO₂ NTs by alternately immersing the latter into 5 mM Bi(NO₃)₃ and 5 mM KI solutions for 10 s each, respectively. The films were carefully washed with doubly distilled water after each dipping step. After certain cycles of SILAR, the resulting BiOI NFs array/TiO₂ NTs array was dried at room temperature.

Fabrication of the BiOI NFs/TiO₂ NPs/ITO and BiOI coating/TiO₂ NTs Electrodes. 0.1 g TiO₂ powder was dispersed ultrasonically in 20 mL water (the concentration of the suspension is 5.0 mg/mL), and then 40 μL of the suspension was applied onto a piece of freshly cleaned ITO slice with fixed area of ~0.25 cm². After drying in air, the film was sintered in a Muffle furnace at 500 °C for 30 min and finally cooled down to room temperature¹⁴. The BiOI NFs/TiO₂ NPs was then prepared by the successive ionic layer adsorption and reaction (SILAR) approach under the same experimental conditions. To fabricate BiOI coating/TiO₂ NTs, BiOI was coated onto the TiO₂ NTs by an impregnating hydroxylation method using BiI₃ as the precursor²⁶. In a typical synthesis, 0.94 g of BiI₃ was added into 20 mL of absolute ethanol solutions containing 2 drops of 35% HCl. The TiO₂ NTs were first immersed in BiI₃ solution for 30 min followed by a slight rinse with ethanol and then dried in an oven at 80 °C for 1 h to ensure that BiI₃ was adhered to the tube wall uniformly. Subsequently, the TiO₂ NTs were immersed in distilled water, and BiOI was deposited on the nanotube wall by hydroxylation of BiI₃.

Immunoassay development. A chitosan film was firstly coated on the BiOI NFs/TiO₂ NTs to offer abundant -NH₂ that covalently links to the -NH₂ of antibodies via the reaction with glutaraldehyde. Specifically, chitosan (CS) solution (0.5 wt%) was prepared by ultrasonically dissolving CS powder in 1% acetic acid. 20 μL CS solution was dropped on hybrid electrode and dried at 50 °C. After the electrode was washed with 0.1 M NaOH and distilled water, respectively, it was dipped in 5.0% GLD solution diluted in phosphate buffer (pH 7.4) at room temperature for 30 min. The electrode was rinsed with distilled water thoroughly to remove physically adsorbed GLD. Then, 25 μL of 0.1 mg/mL Ab₁ dissolved in 0.01 M PBS (pH 7.4) was spread onto the GLD-activated electrode surface at 4 °C in a moisture atmosphere to avoid evaporation of solvent. After incubation for 16 h, the electrode was rinsed with the washing buffer to remove physically adsorbed Ab₁ and then blocked with 25 μL blocking solution for 2 h at 4 °C to block non-specific binding sites, followed by washing with the washing buffer thoroughly. Next, 25 μL of Ag with different concentrations were dropped onto the Ab₁ modified electrodes for an incubation of 60 min at 37 °C followed by washing with washing buffer. Biotinylated Ab₂-streptavidin-biotinylated GDH was prepared through reaction of 100 μL 0.1 mg/mL streptavidin solution (0.01 M PBS, pH 7.4) with 100 μL 0.1 mg/mL biotinylated GDH solution (0.01 M PBS, pH 7.4) for 30 min at room temperature, followed by



addition of 100 μL 0.1 mg/mL biotinylated Ab₂ solution (0.01 M PBS, pH 7.4) for another 30 min at room temperature. After the binding reaction between Ab₁ and the Ag, the electrodes were allowed for labeling by additional incubation with 25 μL of the obtained biotinylated Ab₂-streptavidin-biotinylated GDH solution for 60 min, and again the electrodes were washed thoroughly with water to remove nonspecifically bound conjugations. Finally, the assembled electrodes were allowed for 30 min incubation at room temperature in the freshly prepared 0.1 M Tris-HCl solution (pH 7.8) containing 10 mM glucose and 10 mM NAD⁺ at room temperature, followed by the respective PEC measurements.

- Gill, R., Zayats, M. & Willner, I. Semiconductor Quantum Dots for Bioanalysis. *Angew. Chem. Int. Ed.* **47**, 7602–7625 (2008).
- Haddour, N., Chauvin, J., Gondran, C. & Cosnier, S. Photoelectrochemical Immunosensor for Label-Free Detection and Quantification of Anti-cholera Toxin Antibody. *J. Am. Chem. Soc.* **128**, 9693–9698 (2006).
- Chen, D., Zhang, H., Li, X. & Li, J. H. Bifunctional Titania Nanotubes for Visible-Light-Activated Photoelectrochemical Biosensing. *Anal. Chem.* **82**, 2253–2261 (2010).
- Long, Y. T., Kong, C., Li, D. W., Li, Y., Chowdhury, S. & Tian, H. Ultrasensitive Determination of Cysteine Based on the Photocurrent of Nafion-Functionalized CdS–MV Quantum Dots on an ITO Electrode. *Small* **7**, 1624–1628 (2011).
- Zhang, X. R., Xu, Y. P., Yang, Y. Q., Jin, X., Ye, S. J., Zhang, S. S. & Jiang, L. L. A New Signal-On Photoelectrochemical Biosensor Based on a Graphene/Quantum-Dot Nanocomposite Amplified by the Dual-Quenched Effect of Bipyridinium Relay and AuNPs. *Chem. Eur. J.* **18**, 16411–16418 (2012).
- Zhang, B. T., Guo, L. H. & Greenberg, M. M. Quantification of 8-OxodGua Lesions in Double-Stranded DNA Using a Photoelectrochemical DNA Sensor. *Anal. Chem.* **84**, 6048–6053 (2012).
- Golub, E., Niazov, A., Freeman, R., Zatspein, M. & Willner, I. Photoelectrochemical Biosensors Without External Irradiation: Probing Enzyme Activities and DNA Sensing Using Hemin/G-Quadruplex-Stimulated Chemiluminescence Resonance Energy Transfer (CRET) Generation of Photocurrents. *J. Phys. Chem. C* **116**, 13827–13834 (2012).
- Yao, W. J. *et al.* Electrogenerated tris(bipyridyl) Ru(II)-/nitrotriacetic-polypyrrole copolymer for the easy fabrication of label-free photoelectrochemical immunosensor and aptasensor: Application to the determination of thrombin and anti-cholera toxin antibody. *Biosens. Bioelectron.* **42**, 556–562 (2013).
- Zhan, W. W., Kuang, Q., Zhou, J. Z., Kong, X. J., Xie, Z. X. & Zheng, L. S. Semiconductor@Metal-Organic Framework Core-Shell Heterostructures: A Case of ZnO@ZIF-8 Nanorods with Selective Photoelectrochemical Response. *J. Am. Chem. Soc.* **135**, 1926–1933 (2013).
- Tang, J., Kong, B., Wang, Y. C., Xu, M., Wang, Y. L., Wu, H. & Zheng, G. F. Photoelectrochemical Detection of Glutathione by IrO₂-Hemin-TiO₂ Nanowire Arrays. *Nano Lett.* **13**, 5350–5354 (2013).
- Zhao, W. W., Wang, J., Xu, J. J. & Chen, H. Y. Energy transfer between CdS quantum dots and Au nanoparticles in photoelectrochemical detection. *Chem. Commun.* **47**, 10990–10992 (2011).
- Zhao, W. W., Tian, C. Y., Xu, J. J. & Chen, H. Y. The coupling of localized surface plasmon resonance-based photoelectrochemistry and nanoparticle size effect: towards novel plasmonic photoelectrochemical biosensing. *Chem. Commun.* **48**, 895–897 (2012).
- Zhao, W. W., Dong, X. Y., Wang, J., Kong, F. Y., Xu, J. J. & Chen, H. Y. Immunogold labeling-induced synergy effect for amplified photoelectrochemical immunoassay of prostate-specific antigen. *Chem. Commun.* **48**, 5253–5255 (2012).
- Zhao, W. W., Zhang, L., Xu, J. J. & Chen, H. Y. Cell surface carbohydrates evaluation via a photoelectrochemical approach. *Chem. Commun.* **48**, 9456–9458 (2012).
- Zhao, W. W., Ma, Z. Y., Yu, P. P., Dong, X. Y., Xu, J. J. & Chen, H. Y. Highly Sensitive Photoelectrochemical Immunoassay with Enhanced Amplification Using Horseradish Peroxidase Induced Biocatalytic Precipitation on a CdS Quantum Dots Multilayer Electrode. *Anal. Chem.* **84**, 917–923 (2012).
- Zhao, W. W., Yu, P. P., Shan, Y., Xu, J. J. & Chen, H. Y. Exciton-Plasmon Interactions between CdS Quantum Dots and Ag Nanoparticles in Photoelectrochemical System and Its Biosensing Application. *Anal. Chem.* **84**, 5892–5897 (2012).
- Zhao, W. W., Ma, Z. Y., Yan, Y. D., Xu, J. J. & Chen, H. Y. In Situ Enzymatic Ascorbic Acid Production as Electron Donor for CdS Quantum Dots Equipped TiO₂ Nanotubes: A General and Efficient Approach for New Photoelectrochemical Immunoassay. *Anal. Chem.* **84**, 10518–10521 (2012).
- Zhao, W. W., Ma, Z. Y., Xu, J. J. & Chen, H. Y. In Situ Modification of a Semiconductor Surface by an Enzymatic Process: A General Strategy for Photoelectrochemical Bioanalysis. *Anal. Chem.* **85**, 8503–8506 (2013).
- Zhao, W. W., Shan, S., Ma, Z. Y., Wan, L. N., Xu, J. J. & Chen, H. Y. Acetylcholine Esterase Antibodies on BiOI Nanoflakes/TiO₂ Nanoparticles Electrode: A Case of Application for General Photoelectrochemical Enzymatic Analysis. *Anal. Chem.* **85**, 11686–11690 (2013).
- Zhao, W. W., Xiong, M., Li, X. R., Xu, J. J. & Chen, H. Y. Photoelectrochemical bioanalysis: A mini review. *Electrochem. Commun.* **38**, 40–43 (2014).
- Wen, Z., Li, C., Wu, D., Li, A. D. & Ming, N. B. Ferroelectric-field-effect-enhanced electroresistance in metal/ferroelectric/semiconductor tunnel junctions. *Nature Mater.* **12**, 617–621 (2013).
- Georgiou, T. *et al.* Vertical field-effect transistor based on graphene–WS₂ heterostructures for flexible and transparent electronics. *Nature Nanotech.* **8**, 100–103 (2012).
- Tang, J. Y., Huo, Z. Y., Brittman, S., Gao, H. W. & Yang, P. D. Solution-processed core-shell nanowires for efficient photovoltaic cells. *Nature Nanotech.* **6**, 568–572 (2011).
- Moriya, M., Minegishi, T., Kumagai, H., Katayama, M., Kubota, J. & Domen, K. Stable Hydrogen Evolution from CdS-Modified CuGaSe₂ Photoelectrode under Visible-Light Irradiation. *J. Am. Chem. Soc.* **135**, 3733–3735 (2013).
- Cheng, H. F., Huang, B. B., Dai, Y., Qin, X. Y. & Zhang, X. Y. One-step synthesis of the nanostructured AgI/BiOI composites with highly enhanced visible-light photocatalytic performances. *Langmuir.* **26**, 6618–6624 (2010).
- Dai, G. P., Yu, J. G. & Liu, G. Synthesis and Enhanced Visible-Light Photoelectrocatalytic Activity of p-n Junction BiOI/TiO₂ Nanotube Arrays. *J. Phys. Chem. C* **115**, 7339–7346 (2011).
- Jiang, J., Zhang, X., Sun, P. B. & Zhang, L. Z. ZnO/BiOI Heterostructures: Photoinduced Charge-Transfer Property and Enhanced Visible-Light Photocatalytic Activity. *J. Phys. Chem. C* **115**, 20555–20564 (2011).
- Hahn, N. T., Hoang, S., Self, J. L. & Mullins, C. B. Spray Pyrolysis Deposition and Photoelectrochemical Properties of n-Type BiOI Nanoplatelet Thin Films. *ACS Nano.* **6**, 7712–7722 (2012).
- Kamat, P. V., Tvrdy, K., Baker, D. R. & Radich, J. G. Beyond Photovoltaics: Semiconductor Nanoarchitectures for Liquid-Junction Solar Cells. *Chem. Rev.* **110**, 6664–6688 (2010).
- Wang, K. W., Jia, F. L., Zheng, Z. & Zhang, L. Z. Crossed BiOI flake array solar cells. *Electrochem. Commun.* **12**, 1764–1767 (2010).
- Beranek, R., Macak, J. M., Gärtner, M., Meyer, K. & Schmuki, P. Enhanced visible light photocurrent generation at surface-modified TiO₂ nanotubes. *Electrochim. Acta.* **54**, 2640–2646 (2009).

Acknowledgments

This work was supported by the 973 Program (2012CB932600), the National Natural Science Foundation of China (Nos. 21327902, 21135003, 21121091 and 21305063), the Natural Science Funds of Jiangsu Province (BK20130553) and the open fund of SKLACL (0205119005).

Author contributions

W.W.Z., J.J.X. and H.Y.C. proposed and designed the project, W.W.Z., Z.L., S.S. and W.W.Z. performed the experiments, J.W. and Z.Y.M. performed characterizations, W.W.Z., J.J.X. and H.Y.C. analyzed data and wrote the manuscript. All the authors participated in discussions of the research.

Additional information

Supplementary information accompanies this paper at <http://www.nature.com/scientificreports>

Competing financial interests: The authors declare no competing financial interests.

How to cite this article: Zhao, W.-W. *et al.* Bismuthoxyiodide Nanoflakes/Titania Nanotubes Arrayed p-n Heterojunction and Its Application for Photoelectrochemical Bioanalysis. *Sci. Rep.* **4**, 4426; DOI:10.1038/srep04426 (2014).



This work is licensed under a Creative Commons Attribution-NonCommercial-NoDerivs 3.0 Unported license. To view a copy of this license, visit <http://creativecommons.org/licenses/by-nc-nd/3.0>